Investigating the Variation of Selected *Kepler* Objects Mid-Transit Times

Çağlar Püsküllü[1,*], Oğuz Öztürk[2]

[1,2]Department of Physics, Faculty of Arts and Sciences, Çanakkale Onsekiz Mart University, Çanakkale, Türkiye
[1,2]Astrophysics Research Center and Ulupınar Observatory, Çanakkale Onsekiz Mart University, Çanakkale, Türkiye

Abstract − We derived minima times from the transit light curves of Kepler-412, Kepler-422, Kepler-427 and Kepler-435 observed by Kepler space telescope, using Kwee and van Woerden method and Gauss function fitting. All data were collected from NASA Exoplanet Archive in PDCSAP format with the **wget** command directly from operating system console. Minima times were determined with two different methods; the first one is **AVE** software which uses Kwee and van Woerden method and second, Gauss function is written in **R** statistical programming platform. We examined the Observed minus Calculated (O-C) diagram of each system separately, modelled them with linear and quadratic functions. We obtained that linear models give best fits for the O-C diagrams. Parameter uncertainties were estimated by using the Maximum Likelihood method. We calculated dominant frequencies without any statistical significance on Lomb-Scargle periodograms limited by Nyquist frequency window, as implied by the false alarm probability, FAP of each object. We extracted the noise and considered them as a scale of the measurement uncertainties. We presented updated light elements of systems and concluded that linear models of O-C diagrams are the best fits to the data.

1. Introduction

Transit timing variation (or variation of mid-transit times) analysis is one of the best ways to discover additional orbiting planet or planets in a star-planet system. The analysis itself is well known, from historical O-C studies which are very successful in revealing the mechanisms, such as light-time effect, orbital decay or growth and magnetic activities from eclipsing binary stars. In this respect, it still attracts attention to answer these important questions in this field.

Kepler provides very precise data which spans four-year of observational period enabling to reveal long-term behaviors of thousands and thousands of objects. We selected four objects, Kepler-412, Kepler-422, Kepler-427 and Kepler-435, which have precise photometric data with some potential to display periodical variations in the mid-transit times. Anyone can reach the data presented as PDCSAP transit light curves (see Section 2.1 for technical details) on NASA Exoplanet Archive (NEA). Various methods can be used for measuring the transit times and their uncertainties, with bundled website applications of NEA or on the data downloaded. We chose Kwee and van Woerden (1956) and Gauss fitting methods to derive them by retrieving the data and analyze the potential variations in the observed-calculated (O-C) mid-transit times of each system by fitting linear, parabolic functions and applying Lomb-Scargle frequency analysis (Scargle, 1982; Lomb, 1976) separately. Statistical significance of the results was checked in detail with various methods explained in

---

[1] cpuskullu@comu.edu.tr

[2] oguzozturk@comu.edu.tr

*Corresponding Author

Section 2. We applied likelihood methods for the error estimations. All calculations were made on our personal computers (PCs).

Our paper is organized as follows: In Section 2, we present the properties of the systems considered in this study. Information on the collected observational data, methods we applied, their frequency analysis and error estimations were given. Section 3 describes our findings about the variations of the mid-transit times and summarizes our work by discussing the properties of the planets we studied. Discussions on the best model representations of the O-C diagrams for each system were presented in the final section.

2. Materials and Methods

As is well known, star-star or star-planet systems have a periodical motion around the common center of mass of the orbit. If the planet should pass in front of the host star in the line of sight of the observer in the limit of the orbital inclination; we should observe the transits. Therefore, we can discuss changes in the flux with time due to transit events. When the light is dimming; we observe a continuous drop in the flux, and it has a minimum on this curve. We call this curve as 'transit light curve' and the time that coincides with the middle point of this curve is called as the 'mid-transit time'.

We measured the mid-transit times with various methods and calculated them with respect to a reference mid-transit time and orbital period. These observed versus calculated data (O-C) were listed to make a time series to determine periodical changes in the orbital motion.

Where the data is more precise, we investigate more accurate period in particularly derived values from the orbital solution. These estimated two parameters, new period, and mid-transit time for one planet, are known as 'light elements' of the system. As we summarized in the last section, despite the expectations, we have not found any evidence about any additional or perturbating planets in the systems we study.

2.1. Observational Data

First studies on orbital solutions of the exoplanets began with ground-based observations, many observational data were collected by many observational projects. One of the first projects, The Transatlantic Exoplanet Survey - TrES (Rabus et al., 2009; Gibson, 2009) can be given as an example for ground-based observations. When we start to discuss space-based observations, we should mention about Ford et al. 2012; Mazeh et al., 2013; Rowe et al., 2014; Holczer et al., 2016; Thompson et al., 2018 and Kane et al., 2019 which are important studies, on especially, the NASA's *Kepler* Space Telescope.

Kepler was fully operational between 2009 and 2013 (launched at the beginning of the year, 2009, 6th March). First images were taken in May 2009 by *Kepler*'s 42 chips integrated high-quality camera (Borucki et al., 2010). After 4-year long observational period, 4424 exoplanetary systems were discovered at the date, 2021/07/17.

We worked on the tables from the Objects of Interest (KOI) Cumulative List to get Presearch-data-conditioned Simple Aperture Photometry (PDCSAP) Time Series using visualizer module on Exoplanet Archive (NEA) as seen on Figure 1.
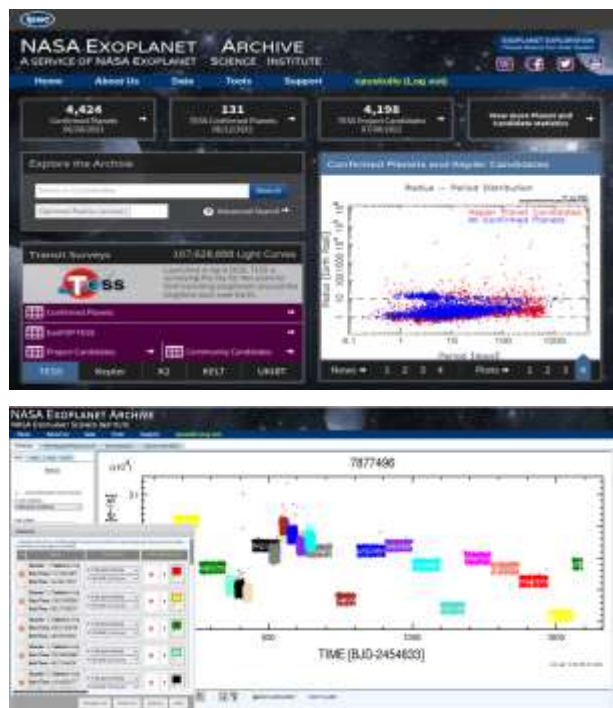
Figure 1. NASA Exoplanet Archive main page and search box (upper panel) and graphical data panel of the object, Kepler-412 (lower panel).

The data was retrieved in the text format with **wget** commands (Foundation, F. S., 2010) provided directly from operating system console. We created their light curves on our PCs with some programming scripts which were written in **R** statistical programming language (R Core Team, 2021). The retrieved text files include three columns: time (BJD), flux (PDCSAP_Flux) and its error. There are two different types of data classified according to the exposure time. These data types are "long cadence" (LC: 30 minutes integration time) and "short cadence" (SC: 59.8 seconds integration time). In this study, we preferred to use the data from the quarters, for which SC data is available, by applying a normalization process to correct the light level of each quarter separately. This choice of SC data decreased the number of points significantly but improved the accuracy and precision because the mid-transit times from LC data will not be adequate for the purpose.

We selected four objects, Kepler-412, Kepler-422, Kepler-427 and Kepler-435 from NEA database after a search for good quality data in a buck of objects listed as less investigated.

2.2. Mid-Transit Timing Measurements

There are many different methods to measure mid-transit times from a light curve. We select Kwee and van Woerden (1956) method, which measurements were done by a very user-friendly software **AVE** (Analysis of Estellar Variablity; Barberá, 1996) developed by Grup d'Estudis Astonomics in Spain while the other methods are still useful such as Gauss-function fitting, polynomial, Fourier and cubic-spline fitting, etc. Successively, we continue to use AVE; however, we considered Gauss function fitting as a second approach by using an **R** script code we developed. We may also mention about the other plot reader software packages used in the field, such as Minima25 (Nelson, 2018), Cepheus-1 (Suhora Observatory, 2018) and Peranso 2 (Vanmunster, 2007). Users can also employ sophisticated modeling software's such as EXOFAST (Eastman et al., 2013), JKTeBOP (Southworth et al., 2008), Juliet (Espinoza et al., 2019), Allestitter (Günther and Daylan, 2022), which provide the mid-transit times as well.

AVE is basically a plotting software which uses a graphical interface to measure the minima times on the plot, loaded in text only formatted data files. The program has an ability, limiting the transit curve to detect the minimum precisely by selected end points of the profile with mouse clicks. AVE makes its profile minimum measurements based on Kwee-van Woerden method. The method can only predict the mid-transit time while the given data is symmetrically and evenly distributed. In this respect, a user will follow this algorithm for

AVE, step by step: 1) The researcher will select an interval using the graphical user interface (GUI) to begin fitting a quadratic equation to the distribution. 2) Software will measure the peak of the hill which shows the minimum of the parabola at the given interval (Kwee - van Woerden method). 3) The given result will be recorded with the errors derived from its simple, geometric technique based on folding a symmetric profile.

Prefered second fitting method is Gauss function, are given by Eq 2.1,

$$g(t) = Ae^{\frac{-(t-\mu)^2}{2\sigma^2}}$$
(2.1)

where t is time, A is amplitude, σ is width of the Gauss curve and μ is defined as mid-transit time. The errors estimated here were given by standard deviation (von Essen et al. 2020).

2.3. O-C Diagram and Lomb-Scargle Frequency Analysis

Lomb-Scargle periodograms are evaluated to investigate if there is a dominant periodical variation in nonuniformly distributed O-C diagrams (Lomb 1976, Scargle 1982). The standard periodogram equation (Eq. 2.2) is given by Scargle (1982), describes providing power for each frequency, to extract time shift of τ, predicted from modulation curves of orthogonal sine-cosine functions which include selected time samples t_i. Afterall, we can write the equation of power, P as a function of the independent parameter, angular frequency ω,

$$P_x(\omega) = \frac{1}{2}\left(\frac{\left[\sum_j X_j \cos(t_j - \tau)\right]^2}{\left[\sum_j \cos^2(t_j - \tau)\right]} + \frac{\left[\left[\sum_j X_j \sin(t_j - \tau)\right]^2\right]}{\left[\sum_j \sin^2(t_j - \tau)\right]} \right)$$
(2.2)

where the time delay, τ

$$tan2\omega\tau = \frac{\sum_j \sin 2\omega t_j}{\sum_j \cos 2\omega t_j}$$
(2.3)

The periodical oscillation (Eq 2.3), ω of each frequency is a parameter of classical wave function (Eq 2.4),

$$\emptyset(t) = A\sin\omega t + B\cos\omega t$$
(2.4)

Hereafter, the limit of the frequency window will be dependent on the Nyquist frequency, $f_{Nyquist} = \frac{1}{2}\upsilon$ where υ is mean frequency.

We can determine the dominant frequencies of each two objects together with their false alarm probabilities (FAP) using Eq 2.5 (Horne and Baliunas, 1986). In this approach, we calculate the noise with Eq 2.6,

$$P_r = \{Z > z\} = 1 - F_z(z) = 1 - [1 - \exp(-1)^N][Z = maks_n P(\omega_n)]$$
(2.5)

where N is random selection in independent frequency number, $P(\omega)$ and z is the power of the frequency,

$$N_i = -6{,}392 + 1{,}193 N_0 + 0{,}00098 N_0{}^2$$
(2.6)

The amplitude of the oscillation ($A_{(O-C)}$) and the epoch ($E_{(O-C)}$) are calculated by selected dominant frequencies. In this respect, to derive these frequencies from resonance periods ($f_{(O-C)}$), we need to model sinusoidal oscillation with nonlinear least square analysis methods (with a package of **R** statistical library called as **NLS**: Douglas and Saikat, 2022),

$$T_{mid-transit} = T_0 + P \times E + A_{(O-C)} \sin 2\pi \frac{E - E_{(O-C)}}{P_{(O-C)}} \tag{2.7}$$

The resonances of the sinusoidal oscillation that we want to find, in other words, variation of the amplitude and the phase of the orbital solution are related to the perturbation, due to the third body and the orbital eccentricity (Lithwick et. al, 2012; Maciejewski et al., 2011; Fukui et al., 2011; Mazeh et al, 2013).

Since we have not probed a statistically significant peak during the frequency analysis, we excluded the sinusoidal variation, and continued with fitting 1st and 2nd degree functions to the O-C diagrams (given by Eq.2.13 and Eq.2.14).

2.4. Error Estimation with Maximum Likelihood method

The formal fitting errors of the transit times can be underestimated with respect to the expected while there are still additional observational and instrumental noise. In this situation we arguably consider the red noise (jitter) and its effect on the observations systematically (Pont et al., 2006, Winn, 2008, Petrucci et al. 2015). When the errors are underestimated, the problem should be solved by isolating red noise (s_i) from each observational mid-transit times error estimation (σ_i):

$$\omega_i = \frac{1}{\sigma_i^2 + s_i^2} \tag{2.8}$$

where the terms ω_i are the weighted errors in the given (Eq 2.8). To obtain additional variance, s_i^2 of each value of residuals, we will use Maximum Likelihood Method – MLM method, suggested by Collier Cameron et al. (2006) and Haywood et al. (2016) and we will get a probability function (Eq. 2.9) for the O-C dataset:

$$\ln(L) = \frac{-n}{2} \ln(2\pi) - \frac{1}{2}\chi^2 - \frac{1}{2}\sum_{i=1}^{N} \ln(\sigma_i^2 + s_i^2) \tag{2.9}$$

where $\chi2$ (chi-squared) is defined as (Eq 2.10),

$$\chi^2 = \sum_i \frac{(y_{0,i} - y_{c,i})^2}{\sigma_i^2 + s_i^2} \tag{2.10}$$

where $y_{0,i}$ and $y_{c,i}$ are the observational and modelled O-C values. To obtain the values of maximum probability, we have to derivate the *ln* (*L*) equation (Eq 2.9) respect to s_i until its limit converges to zero (Eq 2.11).

$$\frac{\partial \ln(L)}{\partial s_i} = 2s_i\left(\sum_i \frac{1}{\sigma_i^2 + s_i^2} - \sum_i \frac{(y_{0,i} - y_{c,i})^2}{\sigma_i^2 + s_i^2}\right) = 0 \tag{2.11}$$

Each equation was solved to obtain additional variance values (s_i)^2:

$$\sum_i \frac{1}{\sigma_i^2 + s_i^2} - \sum_i \frac{(y_{0,i} - y_{c,i})^2}{[\sigma_i^2 + s_i^2]^2} = 0 \tag{2.12}$$

Errors estimated from the linear (Eq 2.13) and quadratic equations (Eq 2.14) which are given for the O-C as

$$T_{mid-transit} = T_0 + P \times E \tag{2.13}$$

$$T_{mid-transit} = T_0 + P \times E + c \times E^2 \tag{2.14}$$

where T_0, P, E and c, respectively, are the reference mid-transit time, orbital period, epoch number (or phase) and the second-degree constant, c gives the rate of the secular change in the orbital period.

We used Akaike Information Criterion (AIC, Akaike 1974, Eq. 2.15) and Bayesian Information Criterion (BIC, Schwarz 1978, Eq 2.16) to decide which model and measurement technique are the best:

$$AIC = -2 \ln L + 2k \tag{2.15}$$

$$BIC = -2 \ln L + k \ln(N) \tag{2.16}$$

where the constant k is the estimated parameter number and N is total number of the mid-transit times.

Using the equations 2.13 and 2.14 and two-measurements methodologies explained after them; we updated the linear ephemeris of the studied systems. When we discuss information criteria (ICs) obtained in this study: we interpret the results in two different ways. Comparing AIC and BIC values of the models provide information on which of the linear and quadratic models should be favored. We also check the significance of the second-degree constant, σ_c obtained from quadratic models as another confidence test. c is the coefficient of the quadratic term and gives the rate of secular change in the orbital period (Öztürk ve Erdem, 2019).

3. Results and Discussion

In this study, we obtained transit light curves of Kepler-412, Kepler-422, Kepler-427 and Kepler-435 from the *Kepler* Exoplanet Data Archive. The minimum times were determined by two different methods. First, based on Kwee and van Woerden; by making use of the **AVE** software. Second by Gauss function-fitting in **R**. To get an orbital solution in our study, we applied linear (Eq. 2.13) and quadratic equations (Eq. 2.14) to the O-C. We didn't consider sinusoidal modelling, because there were no statistically significant peaks in our periodograms, according to frequency analysis. Consequently, we obtained the following results presented in the subsections of this section for each individual system we studied.

3.1.Kepler-412 b

Kepler-412 is a solar analogue (5750 K) star which has a mass of $M_\star = 1.167\ M_\odot$ and a radius of $R_\star = 1.287\ R_\odot$. The measured orbital period of $P = 1.720861232 \pm 4.7\times10^{-8}$ days and its planet has a mass of $M_g = 0.94\ M_J$ and a radius of $R_g = 1.34\ R_J$ (Deleuil ve ark., 2014).

Linear and quadratic models for the O-C diagram are plotted in Figures 2 and 3, the mid-transit times derived with Kwee - van Woerden and Gaussian fitting are given with their uncertainties in Table 1. We describe the terms of each column given Table 1, reference mid-transit time (T_0), period (P), second-degree constant (c) and their significances, respectively. In the last column, we provide two statistics we used for model comparison, which are the values of Akaike Information and Bayesian Information Criteria (AIC and BIC). The results of the frequency analysis are given with the Figure 4.

Second-degree constanst of the quadratic model is 5 σ out of the significance levels of both for Kwee-van Woerden and Gauss fitting, therefore they were not found to be statistically significant.

Table 1
Best fitting MLM parameters of Kepler-412 b. The coefficients of the model parameters are given in each column: updated reference mid-transit time (T_0), period (P), second-degree constant (c) and their significances, respectively. The last column shows two indicators for model comparison which are Akaike and Bayesian Information Criteria (AIC and BIC).

Model	T_0	P	c	Significance of c	AIC/BIC
	(BJD$_{TDB}$ – 2458833)	(days)	(days $\times 10^{-9}$)	(σ)	
Kwee and van Woerden (1956)					
Lineer Model	520.21468 (5)	1.7208593 (8)	---	---	-641.61/-641.35
Quadratic Model	520.21488 (66)	1.720858 (7)	3.35 (15.02)	0.223	-631.77/-631.38
Gauss Fit					
Lineer Model	520.21475 (5)	1.7208595 (7)	---	---	-690.86/-690.58
Quadratic Model	520.21468 (66)	1.720862 (7)	-4.25 (15.13)	0.281	-684.59/-684.18

c: quadratic term.
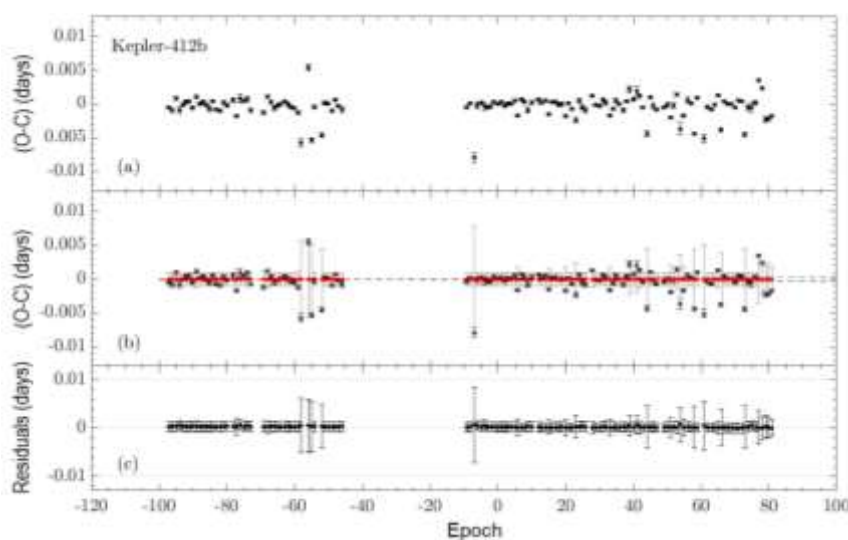
Figure 2. O-C diagram derived from the mid-transit times of Kepler-412 b (black data points with the error bars) calculated by using the Kwee and van Woerden method (a) O-C diagram without the linear fit with MLM method (b) O-C diagram and the linear model obtained with the MLM method (red dots) (c) Residuals of the linear model.
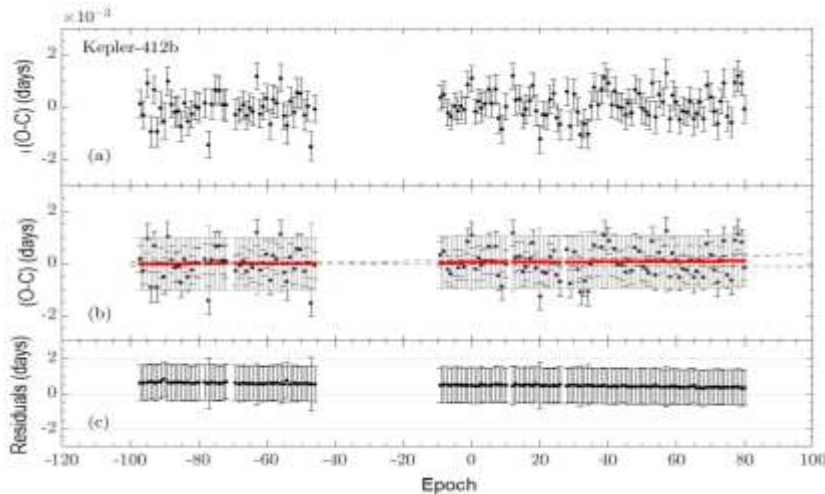
Figure 3. O-C diagram and results of the Gauss fit (for detailed information, please check the Fig.2).
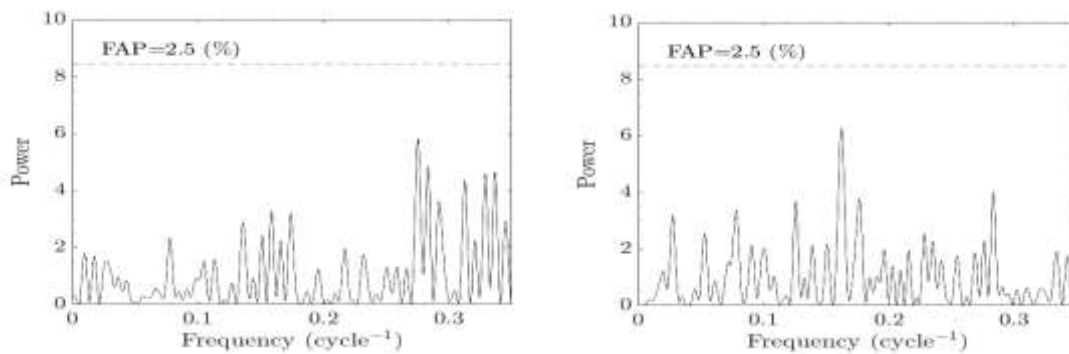
Figure 4. Lomb-Scargle (L-S) periodograms of the O-C data evaluated here, output from (a) **AVE** (b) Gauss fitting method.

3.2. Kepler-422 b

Kepler-422 has a mass of $M_\star = 1.150\,M_\odot$ and a radius of $R_\star = 1.240\,R_\odot$. It's measured temperature is 5972 K. The masses and radii of its planet derived by Endl et al. (2014) are $M_g = 0.43\,M_J$ and radius of $R_g = 1.15\,R_J$. They observed the planet is orbiting with a period of $P = 7.8914483 \pm 5\times10^{-7}$ days.

Linear and quadratic models for the O-C diagram are plotted in Figures 5 and 6, for the mid-transit times derived with Kwee - van Woerden and Gaussian fitting, respectively and their results are given in Table 2. We describe the terms of each column given Table 2, reference transit time (T_0), period (P), second-degree constant (c) and their significances, respectively. In the last column, we provide two statistics we used for model comparison, which are the values of Akaike Information and Bayesian Information Criteria (AIC and BIC). The results of the frequency analysis are given with the Figure 7.

Second-degree constant of the quadratic model was found to be in 1 σ for Kwee-van Woerden fitting, which is significant for Kwee-van Woerden fitting. However c was measured is almost 9 σ which is out of the significance levels for Gauss fitting.

Table 2
Best fitting MLM parameters of the Kepler-422b.

Model	T_0	P	c	Significance of c	AIC/BIC
	(BJD$_{TDB}$ – 2458833)	(days)	(days $\times 10^{-9}$)	(σ)	
Kwee and van Woerden (1956)					
Lineer Model	745.43433 (4)	7.8914480 (10)	---	---	-581.64/-581.52
Quadratic Model	745.43441 (6)	7.8914477 (11)	-56.55 (29.29)	1.931	-579.53/-579.35
Gauss Fit					
Lineer Model	745.43441 (5)	7.8914494 (11)	---	---	-577.54/-577.42
Quadratic Model	745.43442 (7)	7.8914495 (11)	-3.34 (30.48)	0.110	-575.53/-575.35

c: quadratic term constant
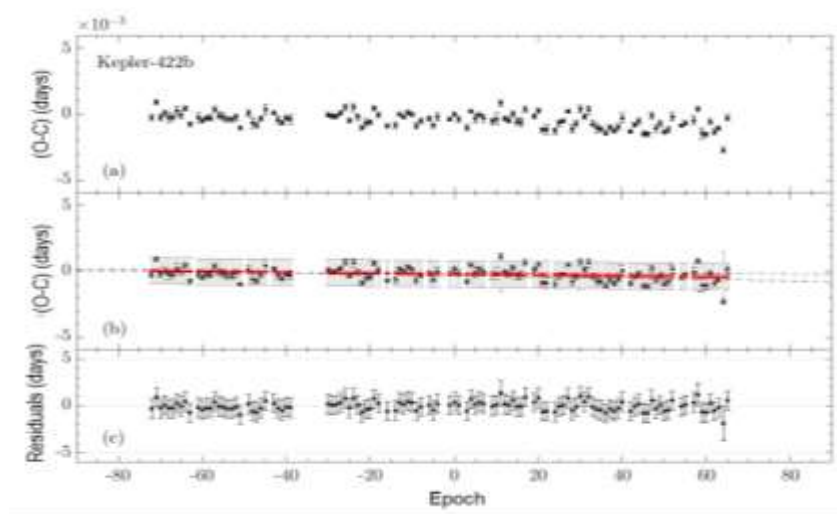
Figure 5. O-C diagram derived from the mid-transit times of Kepler-422 b (black data points with the error bars) calculated by using the Kwee and van Woerden method (a) O-C diagram without the linear fit with MLM method (b) O-C diagram and the linear model obtained with the MLM method (red dots) (c) Residuals of the linear model.
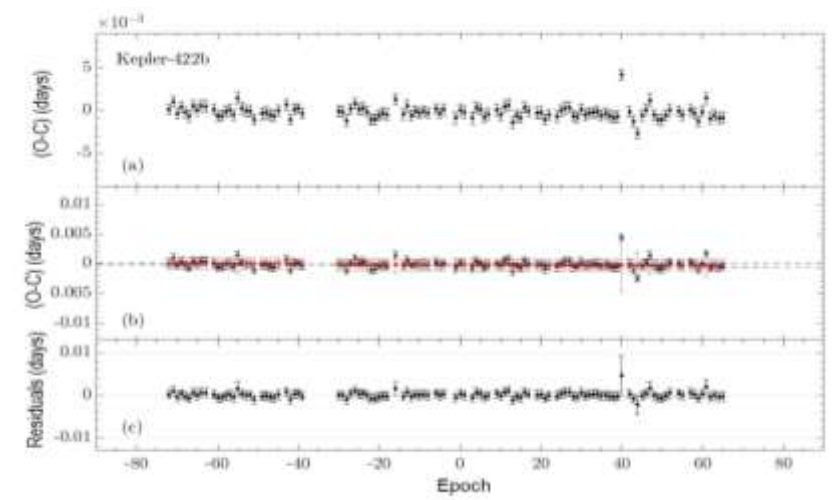
Figure 6. O-C diagram and results of the Gauss fit (detailed information given by Fig.2).
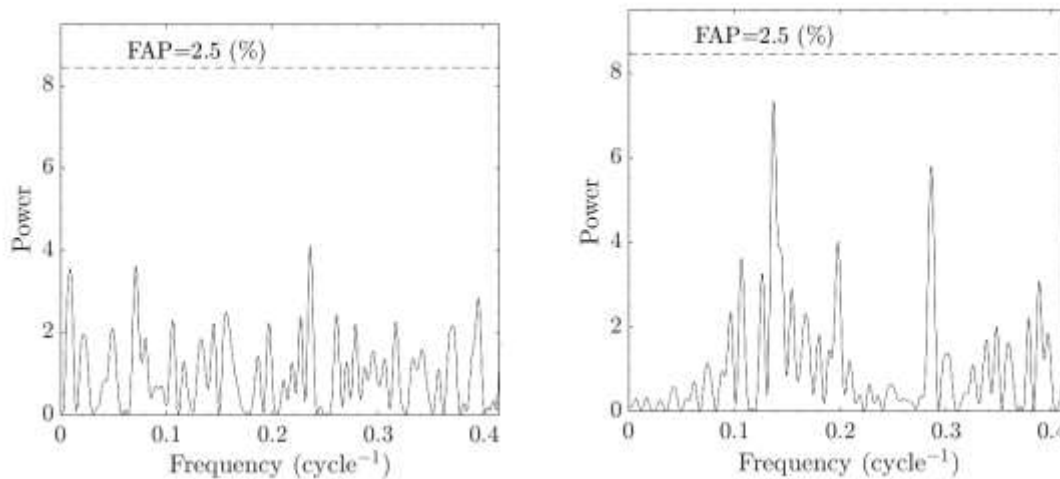
Figure 7. Lomb-Scargle (L-S) periodograms of the O-C data evaluated here, output from (a) **AVE** (b) Gauss fitting method.

3.3. Kepler-427 b

Kepler-427 has a mass of $M_\star = 0.96\ M_\odot$ and a radius of $R_\star = 1.35\ R_\odot$. The orbital period is calculated to be $P = 10.290994 \pm 1.1 \times 10^{-6}$ days of the planet while its measured mass is $M_g = 0.29\ M_J$ and radius is $R_g = 1.23\ R_J$ (Hébrard et al., 2014). In some cases, appeared in Kepler-427, the transit depth can change with degenerations of the planet body reliability (Bierksteker and Schlichting, 2017). In some cases, such as Kepler-427 b, the transit depth can change due to the degeneration in the derived planet parameters (Bierksteker and Schlichting, 2017). In such situations, we added an additional error for the transit time measurements as explained in Section 3.2.

Linear and quadratic models for the O-C diagram are plotted in Figures 8 and 9, for the mid-transit times derived with Kwee - van Woerden and Gaussian fitting, respectively and their results are given in Table 3. We describe the terms of each column given Table 3, reference transit time (T_0), period (P), second-degree constant (c) and their significances, respectively. In the last column, we provide two statistics we used for model comparison, which are the values of Akaike Information and Bayesian Information Criteria (AIC and BIC). The results of the frequency analysis are given with the Figure 10.

Second-degree constant of the quadratic model was found to be in 1 σ for Kwee-van Woerden fitting, which is significant for Kwee-van Woerden fitting. However c was measured is almost 7 σ which is out of the significance levels for Gauss fitting.

Table 3
Best fitting MLM parameters of the Kepler-427b.

Model	T_0	P	c	Significance of c	AIC/BIC
	(BJD$_{TDB}$ – 2458833)	(days)	(days × 10^{-9})	(σ)	
Kwee and van Woerden (1956)					
Linear Model	528.07955 (9)	10.290997 (9)	---	---	-108.23/-109.54
Quadratic Model	528.07965 (14)	10.290993 (10)	-1905.12 (1106.13)	1.723	-106.45/-108.43
Gauss Fit					
Lineer Model	528.07967 (12)	10.290995 (12)	---	---	-107.61/-108.93
Quadratic Model	528.07963 (19)	10.290992 (13)	217.33 (1414.96)	0.154	-105.62/-107.59

c: quadratic term.
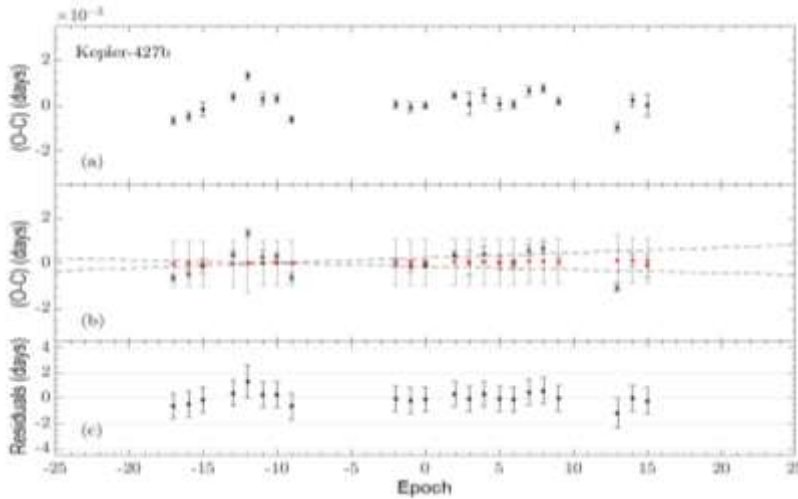
Figure 8. O-C diagram derived from the mid-transit times of Kepler-427 b (black data points with the error bars) calculated by using the Kwee and van Woerden method (a) O-C diagram without the linear fit with MLM method (b) O-C diagram and the linear model obtained with the MLM method (red dots) (c) Residuals of the linear model.
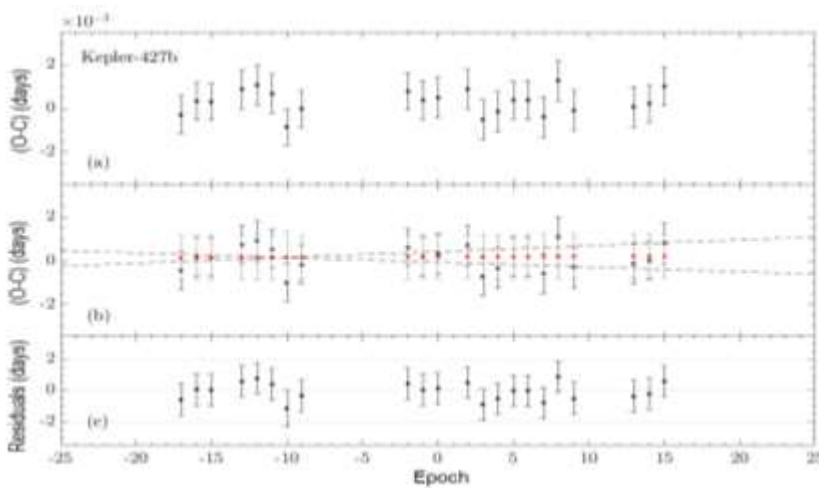
Figure 9. O-C diagram and results of the Gauss fit (detailed information given by Fig.2).
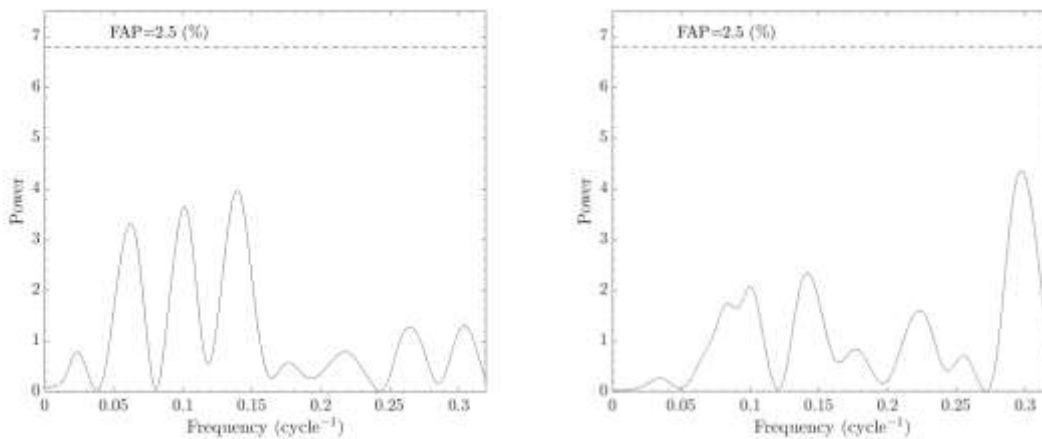
Figure 10. Lomb-Scargle (L-S) periodograms of the O-C data evaluated here, output from (a) **AVE** (b) Gauss fitting method.

3.4. Kepler-435 b

Kepler-435 is a giant with a measured radius of $R_\star = 3.21\ R_\odot$ and a mass of $M_\star = 1.54\ M_\odot$. The orbital period is $P = 8.6001536 \pm 1.8 \times 10^{-6}$ days. The planet has a mass of $M_g = 0.84\ M_J$ and radius of $R_g = 1.99\ R_J$ were given by Almenara et al. (2015).

Linear and quadratic models for the O-C diagram are plotted in Figures 11 and 12, for the mid-transit times derived with Kwee - van Woerden and Gaussian fitting, respectively and their results are given in Table 4.

We describe the terms of each column given Table 4, reference transit time (T_0), period (P), second-degree constant (c) and their significances, respectively. In the last column, we provide two statistics we used for model comparison, which are the values of Akaike Information and Bayesian Information Criteria (AIC and BIC). The results of the frequency analysis are given with the Figure 13.

Second-degree constant of the quadratic model was measured lower than 1σ which is significant for Kwee-van Woerden and Gauss fitting. However the number of data points is low, so we might be hitting the low number statistics problem that means, we have not obtained precise model for the quadratic fits.

Table 4
Best fitting MLM parameters of the Kepler-435b.

Model	T_0	P	c	Significance of c	AIC/BIC
	($BJD_{TDB} - 2458833$)	(days)	(days $\times 10^{-9}$)	(σ)	
Kwee and van Woerden (1956)					
Linear Model	796.85348 (8)	8.600160 (3)	---	---	-98.84/-99.97
Quadratic Model	796.85320 (17)	8.600140 (10)	545.15 (257.66)	2.116	-97.01/-98.72
Gauss Fit					
Lineer Model	796.85349 (10)	8.600161 (3)	---	---	-119.63/-120.76
Quadratic Model	796.85336 (21)	8.600152 (13)	382.49 (332.03)	1.152	-117.65/-119.36

c: quadratic term constant
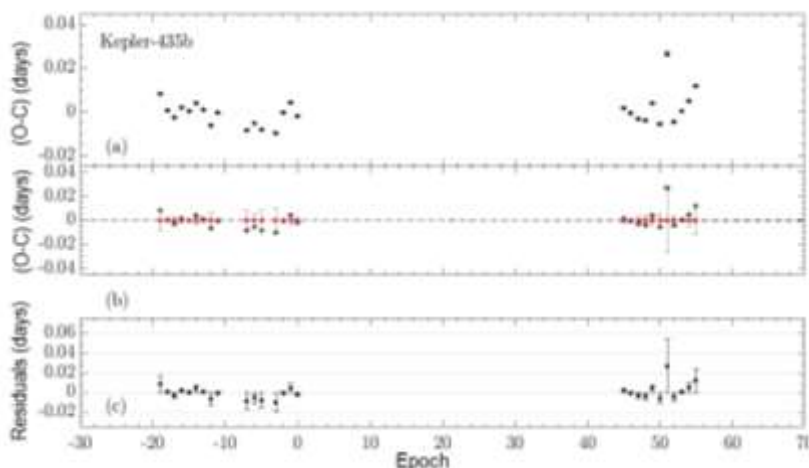
Figure 11. O-C diagram derived from the mid-transit times of Kepler-435 b (black data points with the error bars) calculated by using the Kwee and van Woerden method (a) O-C diagram without the linear fit with MLM method (b) O-C diagram and the linear model obtained with the MLM method (red dots) (c) Residuals of the linear model.
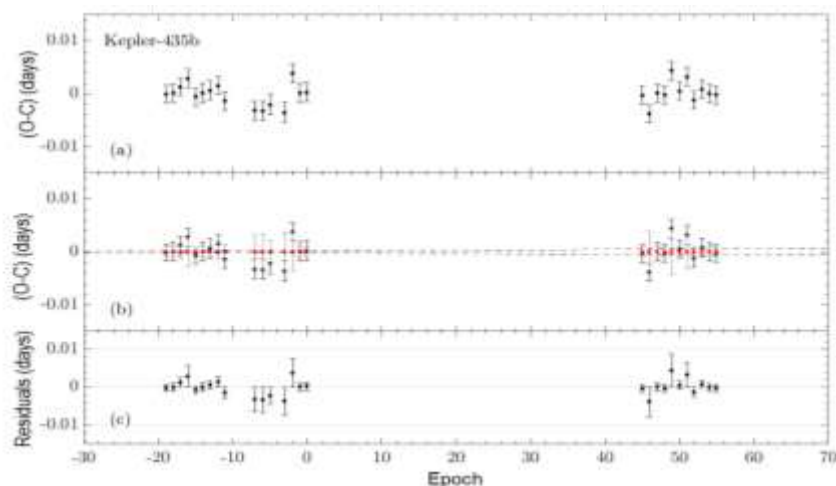
Figure 12. O-C diagram and results of the Gauss fit (detailed information given by Fig.2).
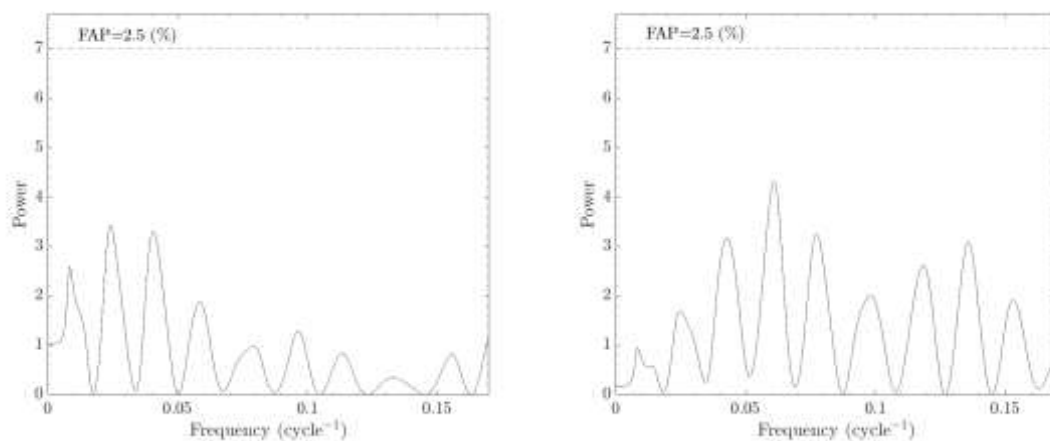
Figure 13. Lomb-Scargle (L-S) periodograms of the O-C data evaluated here, output from (a) **AVE** (b) Gauss fitting method.

The FAPs of the maximum peaks in the power spectra were below the value of 2.5%; which means that we have no evidence for periodical changes in the O-C diagrams. As a result, we updated the linear ephemeris from the linear fits of the O-C diagrams (Table 5).

Table 5
Light elements obtained from linear model.

Object	T_0		P	
	Kwee-van Woerden	Gauss Model	Kwee-van Woerden	Gauss Model
Kepler-412 b	2459353.21468 (5)	2459353.21475 (5)	1.7208593 (8)	1.7208595 (7)
Kepler-422 b	2459578.43433 (4)	2459578.43441 (5)	7.8914480 (10)	7.8914494 (11)
Kepler-427 b	2459361.07955 (9)	2459361.07967 (12)	10.290997 (9)	10.290995 (12)
Kepler-435 b	2459629.85340 (8)	2459629.85349 (10)	8.600160 (3)	8.600161 (3)

4. Conclusion

In this paper, we focused on the results of the (O-C) variation analysis of four Kepler objects' mid-transit times. These objects were well studied by Kane et al., 2009; Ford et al., 2012; Mazeh et al., 2013; Rowe et al.,2014; Holczer et al., 2016 and Thompson et al., 2018 in addition to their discovery papers. We tried to revise the results of their findings on mid-transit times (see Table 5).

O-C diagrams of Kepler-412b can be seen in Figures 3 and 4 for the mid-transit times derived with KW and Gaussian fitting, respectively. Our linear and quadratic models were applied to all O-C datasets separately by using the MLM method. Obtained parameters were presented in Table 1 where we include the second degree constant, *c* derived with high errors over 3 σs. Figures 6 and 7 show O-C diagrams of Kepler-422 b. For this planet, we obtained *c* constant as approximately limits of 1σ according to the Kwee and van Woerden method while its significance is lower than Gauss fitting (Table 2). We present O-C diagrams of Kepler-427 b in the Figures 9 and 10. For this object, we found *c* to be consistent with a constant period within 1 σ based on our measurements with the Kwee-van Woerden method, while its significance is found to be even lower based on the measurements by Gaussian fitting. O-C diagrams of Kepler-435 were given in Figure 12 and 13. We reached the conclusion that second degree *c* constant was not determined precisely for all planets. The secular changes implied by the quadratic fits were not observed within the limits of the uncertainties of the data points (Table 1-4). Comparing the results between AIC and BIC derived from the MLM analysis, we observed that the quality of the fitting is high; We also found that measuring the mid-transit times with Kwee-van Woerden and Gaussian fitting techniques provide similar results.

We concluded that all O-C variations we studied, can be represented with linear models better than quadratic fits, because the estimated errors are even higher than the values of the quadratic coefficients when we employ two different statistical tests. Therefore we reject the quadratic models in each case. We also discussed the measurement quality of our fitting methods: Kwee van Woerden and Gauss function fitting, by comparing with AIC and BIC values? This was the second condition that why we use the ICs. Our results show that there is no statistically signicant difference (see Table 5).

Author Contributions

Çağlar Püsküllü: Retrieved and collected observational data, prepaired it for analysis, performed analysis with the software **AVE** for Kwee-van Woerden method and developed, debugged and applied **R** script for Gauss function to measure mid-transit times, prepared O-C diagrams and perfomed Lomb-Scargle periodagram analysis, wrote and submitted the paper. If you like to study on the code, please get in contact with the author.

Oğuz Öztürk: Retrieved and collected observational data, prepared it for analysis, prepared O-C diagrams and perfomed Lomb-Scargle periodagram analysis with MLM method, reviewed the paper.

Conflicts of Interest

The authors declare no conflict of interest.

References

Agol, E., Steffen, J., Sari, R., and Clarkson, W. (2005). On detecting terrestrial planets with timing of giant planet transits. *Monthly Notices of the Royal Astronomical Society*, 359, 567. DOI: https://doi.org/10.1111/j.1365-2966.2005.08922.x

Akaike, H. (1974). A new look at statistical model identification. System identification and time-series analysis. *IEEE Trans. Automatic Control,* AC-19, 716.

Almenara, J. M., Damiani, C., Bouchy, F., Havel, M., Bruno, G., Hébrard, G., Diaz, R. F., Deleuil, M., Barros, S. C. C., Boisse, I., Bonomo, A. S., Montagnier, G., and Santerne, A. (2015). SOPHIE velocimetry of Kepler transit candidates. XV. KOI-614b, KOI-206b, and KOI-680b: a massive warm Jupiter orbiting a G0 metallic dwarf and two highly inflated planets with a distant companion around evolved F-type stars. *Astronomy and Astrophysics*, 575, A71. DOI: https://doi.org/10.1051/0004-6361/201424291

Barberá, R. (1996). AVE (www.astrogea.org/soft/ave/introave.htm).

Bierksteker, J. B. and Schlichting, H. (2017). Determining Exoplanetary Oblateness Using Transit Depth Variations. *The Astronomical Journal*, 154, 164. DOI: https://doi.org/10.3847/1538-3881/aa88c2

Borucki, W. J. et al. (2010). Kepler Planet-Detection Mission: Introduction and First Results. *Science*, 327, 977. DOI: https://doi.org/10.1126/science.1185402

Collier Cameron, A.; Pollacco, D.; Street, R. A.; Lister, T. A.; West, R. G.; Wilson, D. M.; Pont, F.; Christian, D. J.; Clarkson, W. I.; Enoch, B.; Evans, A.; Fitzsimmons, A.; Haswell, C. A.; Hellier, C.; Hodgkin, S. T.; Horne, K.; Irwin, J.; Kane, S. R.; Keenan, F. P.; Norton, A. J. Parley, N. R.; Osborne, J.; Ryans, R.; Skillen, I.; Wheatley, P. J. (2006). A fast hybrid algorithm for exoplanetary transit searches. *Monthly Notices of the Royal Astronomical Society*, 373, 799. DOI: https://doi.org/10.1111/j.1365-2966.2006.11074.x

Deleuil, M., Almenara, J.-M., Santerne, A., Barros, S. C. C., Havel, M., Hébrard, G., Bonomo, A. S., Bouchy, F., Bruno, G., Damiani, C., Díaz, R. F., Montagnier, G., and Moutou, C. (2014). SOPHIE velocimetry of Kepler transit candidates XI. Kepler-412 system: probing the properties of a new inflated hot Jupiter. *Astronomy and Astrophysics*, 564, A56. DOI: https://doi.org/10.1051/0004-6361/201323017

Douglas M. Bates and Saikat DebRoy (2022): David M. Gay for the Fortran code used by algorithm = "port".

Eastman, J., Gaudi, B. S., Agol, E. (2013). EXOFAST: A Fast Exoplanetary Fitting Suite in IDL. *Publications of the Astronomical Society of Japan,* 125, 923. DOI: https://doi.org/10.1086/669497

Espinoza, N. and Kossakowski, D. and Brahm, R. (2019). Juliet: A Versatile Modelling Tool For Transiting And Non-Transiting Exoplanetary Systems. *Monthly Notices of the Royal Astronomical Society*, 490, 2262-2283. DOI: https://doi.org/10.1093/mnras/stz2688

Endl, M., Caldwell, D. A., Barclay, T., Huber, D., Isaacson, H., Buchhave, L. A., Brugamyer, E., Robertson, P., Cochran, W. D., MacQueen, P. J., Havel, M., Lucas, P., Howell, S. B., Fischer, D., Quintana, E. and Ciardi, D. R. (2014). Kepler-424 B: A Lonely Hot Jupiter That Found A Companion. *The Astrophysical Journal*, 795, 151. DOI: https://doi.org/10.1088/0004-637X/795/2/151

Exoplanet Archive (KOI Cumulative List, 20 Ekim 2020). *https://exoplanetarchive.ipac.caltech.edu/cgi-bin/TblView/nph-tblView?app=ExoTbls&config=cumulative*. DOI: ---

Ford, E. B., Ragozzine, D., Rowe, J. F., Steffen, J. H., Barclay, T., Batalha, N. M., Borucki, W. J., Bryson, S. T., Caldwell, D. A., Fabrycky, D. C., Gautier, T. N., Holman, M. J., Ibrahim, K. A., Kjeldsen, H., Kinemuchi, K., Koch, D. G., Lissauer, J. J., Still, M., Tenenbaum, P., Uddin, K., and Welsh, W. (2012). Transit Timing Observations from Kepler. V. Transit Timing Variation Candidates in the First Sixteen Months from Polynomial Models. *The Astrophysical Journal*, 756, 185. DOI: https://doi.org/10.1088/0004-637X/756/2/185

Foundation, F. S. (2010), Cambridge MA, USA. GNU Wget GNU Wget http://www.gnu.org/software/wget/

Fukui A., Narita N., Tristram P. J., Sumi T., Abe F., Itow Y., Sullivan D. J., Bond I. A., Hirano T., Tamura M., Bennett D. P., Furusawa K., Hayashi F., Hearnshaw J. B., Hosaka S., Kamiya K., Kobara S., Korpela A., Kilmartin P. M., Lin W., Ling C. H., Makita S., Masuda K., Matsubara Y., Miyake N., Muraki Y., Nagaya M., Nishimoto K., Ohnishi K., Omori K., Perrott Y., Rattenbury N., Saito T., Skuljan L., Suzuki D., Sweatman W. L. and Wada K. (2011). Measurements of Transit Timing Variations for WASP-5b. *Publications of the Astronomical Society of Japan.* 63: 287. DOI: https://doi.org/10.1093/pasj/63.1.287

Gibson, N. P.; Pollacco, D.; Simpson, E. K.; Barros, S.; Joshi, Y. C.; Todd, I.; Keenan, F. P.; Skillen, I.; Benn, C.; Christian, D.; Hrudková, M. and Steele, I. A. (2009). A Transit Timing Analysis of Nine Rise Light Curves of the Exoplanet System TrES-3. *The Astrophysical Journal*, 700, 1078. DOI: https://doi.org/10.1088/0004-637X/700/2/1078

Günther, M. N. (2022). Studying exoplanet orbits and dynamics with allesfitter. *European Planetary Science Congress.* EPSC2022-1180. DOI: https://doi.org/10.5194/epsc2022-1180

Haywood, R. D.; Collier Cameron, A.; Unruh, Y. C.; Lovis, C.; Lanza, A. F.; Llama, J.; Deleuil, M.; Fares, R.; Gillon, M.; Moutou, C.; Pepe, F.; Pollacco, D.; Queloz, D. and Ségransan, D. (2016). The Sun as a planet-host star: proxies from SDO images for HARPS radial-velocity variations. *Monthly Notices of the Royal Astronomical Society*, 457, 3637. DOI: https://doi.org/10.1093/mnras/stw187

Hébrard, G., Santerne, A., Montagnier, G., Bruno, G., Deleuil, M., Havel, M., Almenara, J.-M., Damiani, C., Barros, S. C. C., Bonomo, A. S., Bouchy, F., Díaz, R. F. and Moutou, C. (2014). Characterization of the four new transiting planets KOI-188b, KOI-195b, KOI-192b, and KOI-830b. *Astronomy and Astrophysics*, 572, A93. DOI: https://doi.org/10.1051/0004-6361/201424268

Holczer, T., Mazeh, T., Nachmani, G., Jontof-Hutter, D., Ford, E. B., Fabrycky, D., Ragozzine, D., Kane, M., and Steffen, J. H. (2016). Transit Timing Observations from Kepler. IX. Catalog of the Full Long-cadence Data Set. *The Astrophysical Journal Supplement Series*, 225, 9. DOI: https://doi.org/10.3847/0067-0049/225/1/9

Holman, M. J. and Murray, N. W. (2005). The Use of Transit Timing to Detect Terrestrial-Mass Extrasolar Planets. *Science*, 307, 1288. DOI: https://doi.org/10.1106/science.1107822

Horne J. H. and Baliunas S. L. (1986). A prescription for period analysis of unevenly sampled time series. *The Astrophysical Journal.* 302: 757. DOI: https://doi.org/10.1086/164037

Kane, M., Ragozzine, D., Flowers, X., Holczer, T., Mazeh, T. and Relles, H. M. (2019). Visual Analysis and Demographics of Kepler Transit Timing Variations. *The Astronomical Journal*, 157, 171. DOI: https://doi.org/10.3847/1538-3881/ab0d91

Kwee, K. K. and van Woerden, H. (1956). A method for computing accurately the epoch of minimum of an eclipsing variable. Bulletin of the Astronomical Institutes of the Netherlands, 12, 327.

Lithwick Y., Xie J. and Wu Y. (2012). Extracting Planet Mass and Eccentricity from TTV Data. *The Astrophysical Journal.* 761: 122. DOI: https://doi.org/10.1088/0004-637X/761/2/122

Lithwick, Y., Xie, J., and Wu, Y. (2012). Extracting Planet Mass and Eccentricity from TTV Data. *Astrophysics Journal*, 761, 122. DOI: https://doi.org/10.1088/0004-637X/761/2/122

Lomb, N. R. (1976). Least-squares frequency analysis of unequally spaced data. *Astrophysics and Space Science*, 39, 447. DOI: https://doi.org/10.1007/BF00648343

Maciejewski G., Dimitrov D., Neuhäuser R., Tetzlaff N., Niedzielski A., Raetz S., Chen W. P., Walter F., Marka C., Baar S., Krejcová T., Budaj J., Krushevska V., Tachihara K., Takahashi H. ve Mugrauer M. (2011). Transit timing variation and activity in the WASP-10 planetary system. *Monthly Notices of the Royal Astronomical Society.* 411: 1204-1212. DOI: https://doi.org/10.1111/j.1365-2966.2010.17753.x

Mazeh, T.; Nachmani, G.; Holczer, T.; Fabrycky, D.; Ford, E.; Sanchis-Ojeda, R.; Sokol, G.; Rowe, J.; Zucker, S.; Agol, E.; Carter, J.; Lissauer, J.; Quintana, E.; Ragozzine, D.; Steffen, J. and Welsh, W. (2013). Transit Timing Observations from Kepler. VIII. Catalog of Transit Timing Measurements of the First Twelve Quarters. *The Astrophysical Journal Supplement Series*, 208, 16. DOI: https://doi.org/10.1088/0067-0049/208/2/16

Nelson, B. (2018). Minima25 (https://www.variablestarssouth.org/software-by-bob-nelson/).

Öztürk, O.; Erdem, A. (2019). New photometric analysis of five exoplanets: CoRoT-2b, HAT-P-12b, TrES-2b, WASP-12b, and WASP-52b. *Monthly Notices of the Royal Astronomical Society*, 486, 2290. DOI: https://doi.org/10.1093/mnras/stz747

Petrucci, R.; Jofré, E.; Melita, M.; Gómez, M.; Mauas, P. (2015). Transit timing variation analysis in southern stars: the case of WASP-28. *Monthly Notices of the Royal Astronomical Society*, 446, 1389. DOI: https://doi.org/10.1093/mnras/stu2152

Pont, F.; Zucker, S.; Queloz, D. (2006). The effect of red noise on planetary transit detection, *Monthly Notices of the Royal Astronomical Society*, 373, 231. DOI: https://doi.org/10.1111/j.1365-2966.2006.11012.x

Püsküllü, Ç.; Soydugan, F.; Erdem, A.; Budding, E. (2017). Photometric investigation of hot exoplanets: TrES-3b and Qatar-1b. *New Astronomy*, 55, 39. DOI: https://doi.org/10.1016/j.newast.2017.04.001

Rabus, M.; Deeg, H. J.; Alonso, R.; Belmonte, J. A.; Almenara, J. M. (2009). Transit timing analysis of the exoplanets TrES-1 and TrES-2. *Astronomy and Astrophysics*, 508, 1011. DOI: https://doi.org/10.1051/0004-6361/200912252

R Core Team (2021). *R: A language and environment for statistical computing. R Foundation for Statistical Computing*, Vienna, Austria. (https://www.R-project.org/).

Rowe, J. F., Bryson, S. T., Marcy, G. W., Lissauer, J. J., Jontof-Hutter, D., Mullally, F., Gilliland, R. L.,

Issacson, H., Ford, E., Howell, S. B., Borucki, W. J., Haas, M., Huber, D., Steffen, J. H., Thompson, S. E., Quintana, E., Barclay, T., Still, M., Fortney, J., Gautier, T. N., Hunter, R., Caldwell, D. A., Ciardi, D. R., Devore, E., Cochran, W., Jenkins, J., Agol, E., Carter, J. A., and Geary, J. (2014). Validation of Kepler's Multiple Planet Candidates. III. Light Curve Analysis and Announcement of Hundreds of New Multi-planet Systems. *The Astrophysical Journal*, 784, 45. DOI: https://doi.org/10.1088/0004-637X/784/1/45

Scargle, J. D. (1982). Studies in astronomical time series analysis. II - Statistical aspects of spectral analysis of unevenly spaced data. *The Astrophysical Journal*, 263, 835S. DOI: https://doi.org/10.1086/160554

Schwarz,G. (1978). Estimating the Dimension of a Model. *Annuals of Statistics*. 6, 461.

Southworth, J. (2008). Homogeneous studies of transiting extrasolar planets - I. Light-curve analyses. *Monthly Notices of the Royal Astronomical Society*, 386, 1644-1666. DOI: https://doi.org/10.1111/j.1365-2966.2008.13145.x

Suhora Observatory, Retrieved 24.06.2018 from http://www.as.up.krakow.pl/miniauto/.

Thompson, S. E., Coughlin, J. L., Hoffman, K., Mullally, F., Christiansen, J. L., Burke, C. J., Bryson, S., Batalha, N., Haas, M. R., Catanzarite, J., Rowe, J. F., Barentsen, G., Caldwell, D. A., Clarke, B. D., Jenkins, J. M., Li, J., Latham, D. W., Lissauer, J. J., Mathur, S., Morris, R. L., Seader, S. E., Smith, J. C., Klaus, T. C., Twicken, J. D., Van Cleve, J. E., Wohler, B., Akeson, R., Ciardi, D. R., Cochran, W. D., Henze, C. E., Howell, S. B., Huber, D., Prša, A., Ramírez, S. V., Morton, T. D., Barclay, T., Campbell, J. R., Chaplin, W. J., Charbonneau, D., Christensen-Dalsgaard, J., Dotson, J. L., Doyle, L., Dunham, E. W., Dupree, A. K., Ford, E. B., Geary, J. C., Girouard, F. R., Isaacson, H., Kjeldsen, H., Quintana, E. V., Ragozzine, D., Shabram, M., Shporer, A., Silva Aguirre, V., Steffen, J. H., Still, M., Tenenbaum, P., Welsh, W. F., Wolfgang, A., Zamudio, K. A., Koch, D. G., and Borucki, W. J. (2018). Planetary Candidates Observed by Kepler. VIII. A Fully Automated Catalog with Measured Completeness and Reliability Based on Data Release 25. *The Astrophysical Journal Supplement Series*, 235, 38. DOI: https://doi.org/10.3847/1538-4365/aab4f9

Vanmunster, T. (2007). Peranso period analysis software (www.peranso.com).

von Essen, Carolina; Lund, Mikkel N.; Handberg, Rasmus; Sosa, Marina S.; Gadeberg, Julie Thiim; Kjeldsen, Hans; Vanderspek, Roland K.; Mortensen, Dina S.; Mallonn, M.; Mammana, L.; Morgan, Edward H.; Villaseñor, Jesus Noel S.; Fausnaugh, Michael M.; Ricker, George R. (2020). TESS Data for Asteroseismology: Timing Verification. *The Astronomical Journal*, 160, 34. DOI: https://doi.org/10.3847/1538-3881/ab93dd

Winn, J. N. (2008). Precise Photometry and Spectroscopy of Transits Extreme Solar Systems. *ASP Conference Series,* Vol. 398. Retrieved from: https://arxiv.org/abs/0710.1098